J Fluoresc (2015) 25:897–905
DOI 10.1007/s10895-015-1570-9

ORIGINAL PAPER

A Simple Fluorescence Quenching Method for the Determination of Vanillin Using TGA-capped CdTe/ZnS Nanoparticles as Probes

Li Li[1] · Qiaolin Zhang[1] · Yaping Ding[1] · Yaxiang Lu[2] · Xiaoyong Cai[1] · Lurong Yu[1]

Received: 21 January 2015 / Accepted: 10 April 2015 / Published online: 25 April 2015

Abstract Based on the quenching of the fluorescence intensity of thioglycolic acid (TGA)-capped core-shell CdTe/ZnS nanoparticles (NPs) by vanillin, a novel, simple and rapid method for the determination of vanillin was proposed. In aqueous medium, the functionalized core-shell CdTe/ZnS NPs were successfully synthesized with TGA as the capping ligand. TGA-capped core-shell CdTe/ZnS NPs were characterized by using X-ray diffraction (XRD), transmission electron microscopy (TEM) and Fourier transform infrared (FTIR) spectroscopy. Factors affecting the vanillin detection were investigated, and the optimum conditions were also determined. Under the optimum conditions, the relative fluorescence intensity of CdTe/ZnS NPs was linearly proportional to vanillin over a concentration range from 9.4×10^{-7} to 5.2×10^{-4} M with a correlation coefficient of 0.998 and a detection limit of 2.6×10^{-7} M. The proposed method was also employed to detect trace vanillin in cookies with satisfactory results.

Keywords CdTe/ZnS nanoparticles · Core-shell · Fluorescence probe · Vanillin

✉ Li Li
lilidu@shu.edu.cn

✉ Yaping Ding
wdingyp@sina.com

[1] Department of Chemistry, Shanghai University, Shanghai 200444, People's Republic of China

[2] School of Chemical Engineering, University of Birmingham, Birmingham B15 2TT, UK

Introduction

Vanillin (VAN, 4-hydroxy-3-methoxy-benzaldehyde) is one of the most important flavouring agents, which is extracted from the cured beans of Vanilla planifolia [1, 2]. It is widely used to contribute to the fragrance of candies, cosmetic, beverages and pharmaceuticals because of its unique flavor and aroma properties [3, 4]. Moreover, VAN also displays antimicrobial and antioxidant properties [5–7], so it is used as a food preservative in food industry as well. VAN is reported to have beneficial health effects such as inhibiting the oxidation of human low density lipoproteins [8] and inducing an antisickling effect through covalent bonding of the aldehyde group of vanillin molecules with the hemoglobin group in the red blood cells [9]. However, VAN is a synthetic perfume and food additive, excessive ingesting of VAN can cause headaches, nausea, vomiting [10] and even has cocarcinogenic potential when being digested intraperitoneally at high concentration [11]. As a result, it is of great importance to develop a sensitive method for qualitative and quantitative detection of VAN.

Up to now, various methods have been developed for the determination of VAN, including liquid chromatography-mass spectrometry (LC-MS) [12], capillary electrophoresis (CE) [13, 14], electrochemical method [15–17], high performance liquid chromatography (HPLC) [3, 9, 18], gas chromatography-mass spectrometry (GC-MS) [19] and so on. However, these methods mentioned above have their own limits like high cost and complex operation. Compared with these methods, fluorimetry has many advantages like low cost, easy operation, high sensitivity, low detection limit and so on [20]. Accordingly, it is necessary to develop a simple and sensitive method for the determination of VAN.

Luminescent semiconductor nanoparticles (NPs) hold immense promise to use as fluorescence probes [21–23] for

chemical and biomedical applications in the past decades. Semiconductor NPs present a series of excellent optical and chemical properties, such as long-term photostability, broad excitation spectrum, narrow/symmetric emission spectrum, and readily tunable spectra [24, 25]. Surface chemistry plays an important role concerning the properties of NPs [26], and many efforts have been made to improve the surface properties. L-cysteine, TGA, and glutathione (GSH) are commonly used capping ligands for surface modification. However, the application of NPs with a single-core structure has a large amount of limitations. As is reported, the shell has a crucial effect on the fluorescence quantum yield and the photochemical stability of NPs [27]. Therefore, various techniques have been proposed for preparing NPs with a core-shell structure. ZnS, CdS, and ZnSe are common shells grown around cores and among them, ZnS is the most commonly used shell material because it presents better stability and less toxicity than other shell materials [28].

To our knowledge, the use of TGA-capped CdTe/ZnS NPs in the study of the interaction between NPs and VAN by the fluorescent technique has not been reported so far. In the present work, a convenient, sensitive and selective method for quantitative detection of VAN was proposed based on the quenching of the fluorescence of TGA-capped CdTe/ZnS NPs in aqueous solution. The functionalized core-shell CdTe/ZnS fluorescence probes were prepared by using inorganic salts as precursors and TGA as the stabilizer. Under the optimum conditions, it was found that the fluorescence intensity of TGA-capped CdTe/ZnS NPs quenched in the presence of VAN. The quenched fluorescence intensity was proportional to the concentration of VAN. Based on this phenomenon, a new method for the determination of VAN was developed. The method has been applied to the determination of VAN in real samples and satisfactory results were obtained.

Experimental

Reagents

Sodium borohydride (96 %), $Na_2S \cdot 9H_2O$ (analytical purity), tellurium powder (99.999 %), $CdCl_2 \cdot 2.5H_2O$ (analytical purity) and thioglycolic acid (TGA, analytical purity) were acquired from Shanghai Sinopharm Chemical Reagent Co. Ltd. (China). $ZnSO_4 \cdot 7H_2O$ (analytical purity) was purchased from Shanghai Jinshan Chemical Plant (China). VAN was obtained from Aladdin Chemical Reagent Co., Ltd. (Shanghai, China) and cookies were purchased from the local supermarket. All chemicals used are of the highest purity available and all experiments were performed in a phosphate buffer solution (PBS) which was prepared by adjusting 0.1 M K_2HPO_4, KH_2PO_4, H_3PO_4, or NaOH. Doubly distilled water (DDW) was used throughout the experiments.

Apparatus

Powder XRD spectra were recorded on a Rigaku DX-2700 X-ray diffractometer with Cu-Kα radiation (λ=0.15418 nm) (Japan). A JEM-2010F transmission electron microscope (TEM) was used for morphologic characterization. AVATAR 370 Fourier transform infrared (FTIR) spectrophotometer was used to acquire the FTIR spectra, and a UV-2501PC spectrometer (Shimadzu, Japan) was applied to obtain the absorption spectra. The fluorescence spectra were measured with a RF-5301PC spectrofluorometer (Shimadzu, Japan) using a quartz cell with 1.0 cm path length. All pH measurements were conducted with a pHS-3C pH meter (Analytical Instruments Co., Shanghai, China). All optical measurements were carried out at room temperature under ambient conditions.

Synthesis of Water-Soluble TGA-capped CdTe/ZnS Nanoparticles

Water-soluble CdTe/ZnS NPs capped by TGA were prepared according to the literatures reported before [29, 30]. First, the fresh NaHTe solution was synthesized by dissolving 25.5 mg Te powder and 151.2 mg $NaBH_4$ in 5 mL oxygen-free DDW, which reacted about 2 h until the Te powder was completely disappeared. Then, 91.3 mg $CdCl_2 \cdot 2.5H_2O$ was dissolved in 95 mL DDW and 74 μL TGA was added, the pH of which was adjusted to 9–10 by stepwise addition of 1.0 M NaOH solution. The above solution was saturated with N_2 for about 30 min and the fresh NaHTe solution prepared previously was quickly injected into the flask under vigorous stirring. CdTe NPs was obtained after the mixed solution was heated to reflux in a water bath for 1.5 h.

Subsequently, the as-prepared CdTe sample was added to a solution (80 mL, pH=9) that contained $ZnSO_4$ (230 mg) and

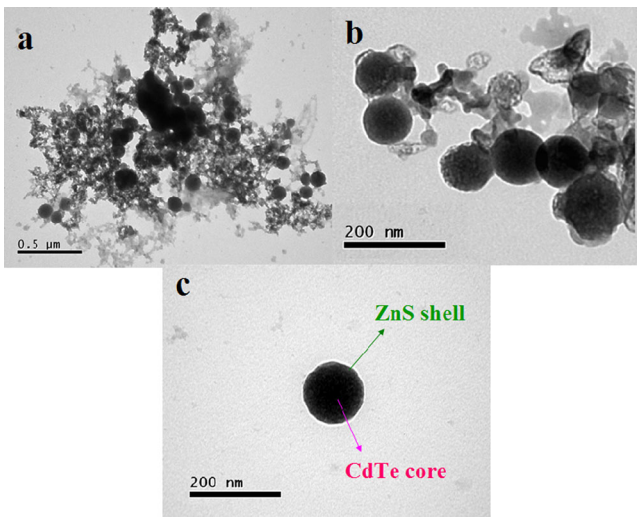

Fig. 1 TEM images of TGA-capped CdTe/ZnS NPs. **a** scale bar: 0.5 μm; **b** and **c**: scale bar: 200 nm

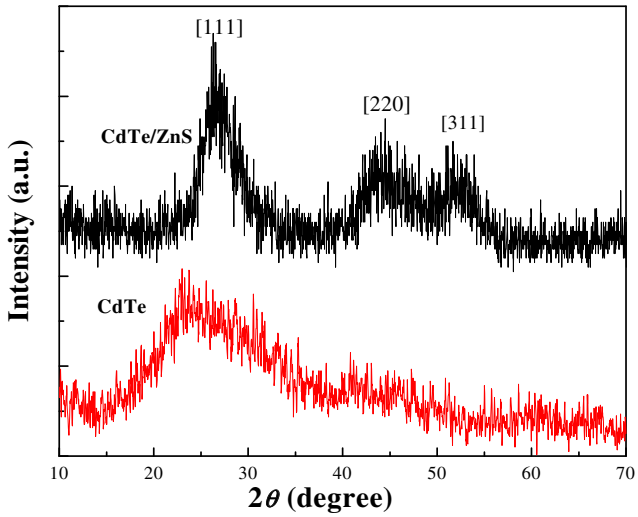

Fig. 2 XRD pattern of TGA-capped CdTe/ZnS NPs

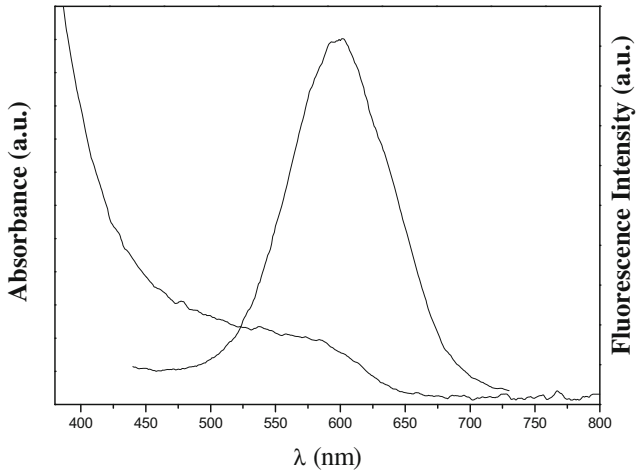

Fig. 4 Fluorescence emission spectrum and UV-vis absorption spectrum of TGA-capped CdTe/ZnS NPs

TGA (148 μL). The mixture was transferred to an oil bath and heated to boil for 8–9 min. During the boiling, Na_2S solution (20 mL) was then added dropwise. After that, the solution was maintained at 60 °C in a water bath to reflux for 1 h to control the sizes of core-shell NPs. Thus, the functionalized core-shell CdTe/ZnS NPs were obtained.

Determination of VAN with Core-Shell CdTe/ZnS Fluorescence Probes

The detection procedures are as follows: in a set of 25 mL calibrated brown volumetric flasks, 300 μL of the as-prepared TGA-capped core-shell CdTe/ZnS NPs solution and a series of different concentrations of VAN standard solutions were added. The mixtures were diluted to the volume with PBS (pH=7.5) solution. The fluorescence spectra were recorded at an excitation wavelength of 374 nm with excitation and emission slits width of 5 nm.

Results and Discussion

Characterization of TGA-capped CdTe/ZnS NPs

The morphology and structure of the prepared TGA-capped core-shell CdTe/ZnS NPs were characterized by TEM and XRD. TEM images were shown in Fig. 1 and it can be found

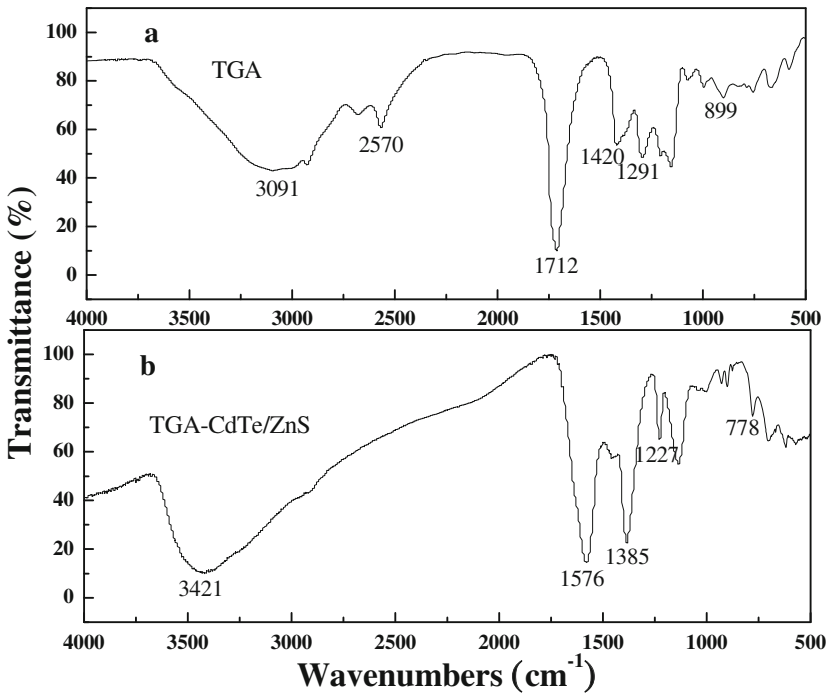

Fig. 3 FT-IR spectra of (**a**) pure TGA and (**b**) TGA capped CdTe/ZnS NPs

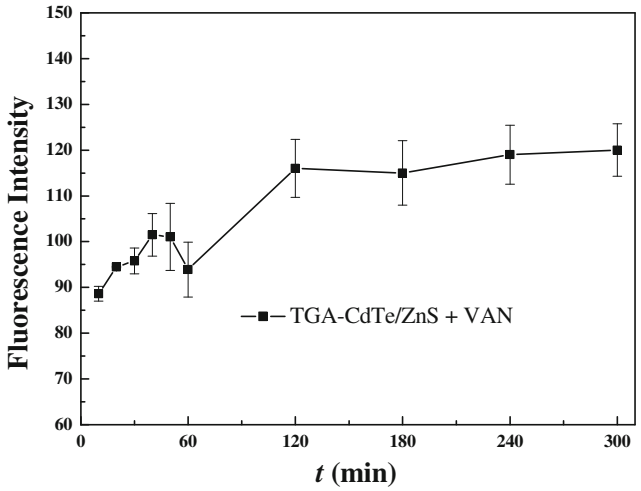

Fig. 5 Effect of reaction time on the fluorescence intensity of TGA-CdTe/ZnS-VAN system

that TGA-capped CdTe/ZnS NPs are most round particles with an average diameter of about 100 nm. In addition, a magnified view in Fig. 1c shows the clear core-shell morphology of TGA-capped CdTe/ZnS NPs.

Figure 2 shows the powder XRD analysis results of TGA-capped CdTe and TGA-capped CdTe/ZnS NPs that were precipitated from an aqueous solution of TGA-capped CdTe and TGA-capped CdTe/ZnS NPs with excess absolute ethyl alcohol. The characteristic zinc blend planes of 111, 220, and 311 located at 24.77°, 41.15°, and 46.10° for the CdTe core and at 26.51°, 43.96° and 52.13° for CdTe/ZnS in the 10–60° 2θ range are observed. After the growth of ZnS shell on the CdTe core, the peak position shifted to higher angles towards the positions of ZnS cubic structures peaks (JCPDS no. 05-0566), which further demonstrated the formation of ZnS shell.

To identify the conjugation mode between TGA and CdTe/ZnS NPs, FTIR spectra of pure TGA and TGA-capped CdTe/ZnS NPs were recorded as shown in Fig. 3. The infrared

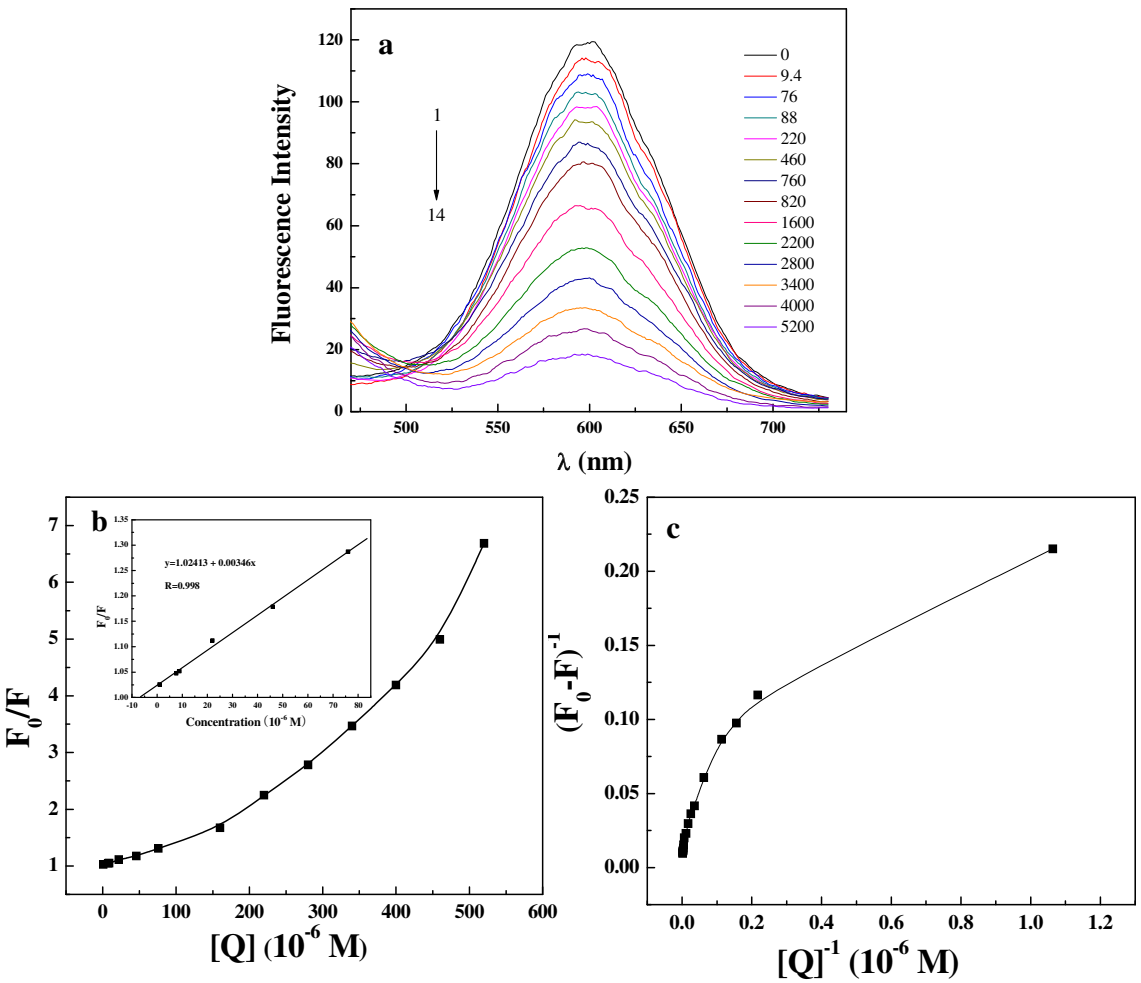

Fig. 6 **a** Fluorescence intensity of TGA-capped CdTe/ZnS NPs in the absence and presence of VAN. C_{VAN} (0.1 μM)=(1) 0; (2) 9.4; (3) 76; (4) 88; (5) 220; (6) 460; (7) 760; (8) 820; (9) 1600; (10) 2200; (11) 2800; (12) 3400; (13) 4000; (14) 5200; **b** Stern–Volmer plot for interaction between TGA-capped CdTe/ZnS NPs and VAN. *Inset* shows linear relationship in the lower concentration ranging from 9.4×10^{-7} to 7.6×10^{-5} M. **c** Lineweaver-Burk plot for interaction between TGA-capped CdTe/ZnS NPs and VAN

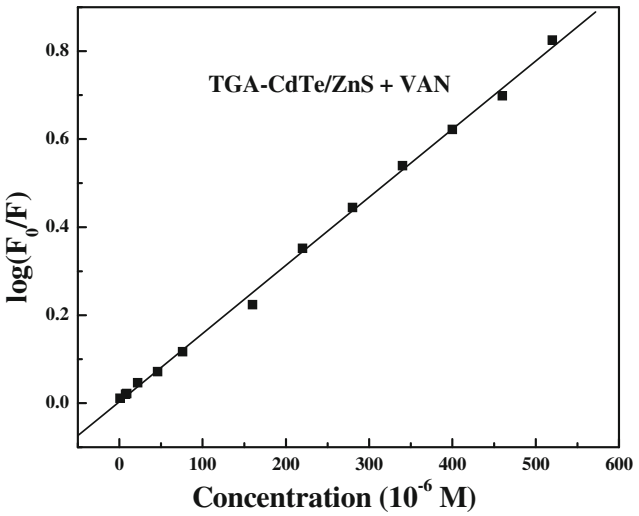

Fig. 7 Modified Stern-Volmer relationship between TGA-capped CdTe/ZnS NPs and VAN

absorption bands of CdTe/ZnS NPs capped with TGA occur at 3421, 1576, 1385, 1227, and 778 cm^{-1}, corresponding to the -OH stretching vibration, COO- asymmetric stretching vibration, COO- symmetric stretching vibration, C=O stretching vibration and C-S stretching vibration, respectively [31]. Comparing Fig. 3a with Fig. 3b, a significant difference was found that the peak of S-H group at 2570 cm^{-1} [32] was absent in TGA-capped CdTe/ZnS NPs. The reason for the disappearance of the S-H group vibration on the surface of CdTe/ZnS NPs was due to the covalent bonding interactions between thiols and the surface of CdTe/ZnS.

TGA-capped CdTe/ZnS NPs were optically characterized by the UV-vis absorption spectra and fluorescence spectra as shown in Fig. 4. It can be seen that the CdTe/ZnS fluorescence probes have a wide range of absorption with a shoulder centers at about 575 nm. The emission spectrum of CdTe/ZnS NPs is narrow and symmetric with the maximum emission wavelength at about 600 nm.

Effect of pH and Reaction Time on the Fluorescence Intensity

pH and reaction time are two most important factors that influence the fluorescence intensity of the VAN-CdTe/ZnS system. It has been documented that NPs are pH sensitive and the pH can influence the metal-ligands complexes on the surface of NPs, thus resulting in the difference in fluorescence quantum yield and surface-related emission of the NPs. Therefore, different reaction environment contributes to the PL change and the stability of the NPs solution. All the measurements were performed in pH 7.5 phosphate buffer solution.

At room temperature, the effect of reaction time on the fluorescence intensity was explored to find the optimum condition, which is shown in Fig. 5. As is seen, the fluorescence intensity became stable after reacting for 2 h. Therefore, the fluorescence intensity was recorded after the system reacted for 2 h.

Table 1 Effect of coexisting foreign substances on fluorescence intensity of TGA-capped CdTe/ZnS NPs (concentration of vanillin was 4×10^{-6} M, room temperature)

Coexisting substance	Mole ratio ($C_{species}/C_{VAN}$)	Change in FL intensity to VAN (%)
Mg^{2+}, SO_4^{2-}	5	−0.15
Na^+, Cl^-	30	−0.98
K^+, NO_3^-	10	+4.69
NH_4^+, Cl^-	30	+3.5
Zn^{2+}, SO_4^{2-}	5	−1.18
Glucose	30	+1.93
Sucrose	10	+2.04
Maltose	15	+2.52
Citric acid	10	−3.18
Benzoic acid	20	−3.26
Ascorbic acid	20	+4.96
Caffeine	10	+1.62
L-cysteine	3	+10.26
L-arginine	20	+4.71
L-alanine	10	+4.85

Determination of VAN with TGA-capped CdTe/ZnS NPs

Under the optimal conditions mentioned above, the emission spectra of TGA-capped CdTe/ZnS NPs under different amount of VAN were recorded. As is shown in Fig. 6a, VAN has a tremendous impact on the fluorescence emission of TGA-capped CdTe/ZnS NPs. It was found that the fluorescence intensity of TGA-capped CdTe/ZnS NPs decreased in the presence of VAN. Moreover, it is observed that the quenching effect is concentration-dependent, which demonstrates that TGA-capped CdTe/ZnS NPs have the potential to be sensitive probes for determination of VAN.

As is known, there are two types of quenching for describing the interaction between quencher and fluorophores: dynamic and static. If the quenching is dynamic, the linear plot will follow the Stern-Volmer equation. If the quenching is

Table 2 Determination of vanillin in cookies by the proposed method

Number	Added (μM)	Found (μM)	Recovery (%)	RSD (%)
1	10	9.7	97.0	1.5
2	24	23.9	99.6	3.2
3	30	30.7	102.3	2.8

Table 3 Comparison of the performances of different methods

Methods	Linear range (μM)	Detection limits (μM)	References
Voltammetric method	0.1-7, 10–40	0.02	[10]
LC-MS	2.5×10^{3}–5.6×10^{4}	–	[12]
Chemiluminometric	0.99–65.7	0.30	[38]
square-wave voltammetry	–	0.4	[15]
Spectrophotometric	6.5–131	3.2	[39]
Adsorptive Stripping Voltammetry	3.3–9.8	0.16	[40]
Fluorescenc probes	0.94–520	0.26	Present method

static, the linear plot will follow the Lineweaver-Burk equation.

The dynamic quenching effect of VAN can be described using the following Stern-Volmer equation [33, 34]:

$$F_0/F = K_{SV}[Q] + 1$$

where F_0 and F are the fluorescence intensities of the TGA-capped CdTe/ZnS NPs in the absence and presence of VAN, respectively. *[Q]* represents the concentration of VAN, and K_{SV} is the Stern-Volmer quenching constant. As shown in the inset of Fig. 6b, the Stern-Volmer plot of (F_0/F) versus *[Q]* shows a good linear relationship (R=0.998) for VAN concentration in the range from 9.4×10^{-7} to 7.6×10^{-5} M and the quenching constant (K_{SV}) of TGA-capped CdTe/ZnS NPs with VAN could be calculated as 3.46×10^{3} M^{-1}. If experimental data follow the Stern-Volmer equation, the plot of F_0/F versus *[Q]* should be linear. However, in this work, it was found that the quenching of fluorescence of TGA-capped CdTe/ZnS NPs did not obey to the typical linear Stern-Volmer plot in the higher concentration ranges.

The static quenching effect can be described using Lineweaver-Burk equation as follows [35, 36]:

$$(F_0-F)^{-1} = F0^{-1} + K_D{}^{-1}F_0{}^{-1}[Q]^{-1}$$

where K_D is the binding constant. As shown in Fig. 6c, the Lineweaver-Burk plot of $(F_0\text{-}F)^{-1}$ versu $[Q]^{-1}$ *don't* show a linear relationship for VAN concentration in the range of 9.4×10^{-7}-5.2×10^{-4} M, which demonstrates that both dynamic and static quenching modes act together in this system.

Calibration Curve and Detection Limit

To further discuss the quenching effect of TGA-capped CdTe/ZnS NPs on VAN, a modified Stern-Volmer equation was utilized to gain a calibration plot, which was proposed for the systems involving both static and dynamic quenching mechanism. It could be shown as follows [37]:

$$log(F_0/F) = K_{SV}[Q] + C$$

where C is a constant. In this investigation, the K_{SV} and C can be calculated as 1.55×10^{3} M^{-1} and 0.0035, respectively. As is shown in Fig. 7, the calibration plot of $log(F_0/F)$ versus *[Q]* shows a rather good linear relationship for VAN concentration in the range of 9.4×10^{-7}–5.2×10^{-4} M (correlation coefficient, R^2=0.998). The detection limit calculated using the equation 3σ/S (where σ is the standard deviation of blank measurements of six replicates and S is the slope of the calibration curve) is 2.6×10^{-7} M.

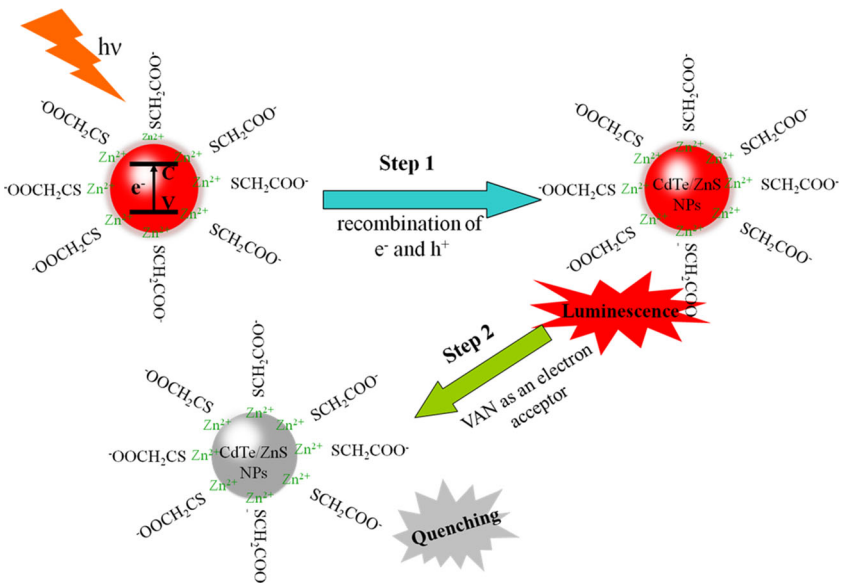

Scheme 1 Mechanism of fluorescence quenching of TGA-capped CdTe/ZnS NPs in the presence of VAN

Tolerance of Foreign Substances

In order to study the selectivity of the proposed method, the interference of foreign species was carried out by preparing solutions containing 4×10^{-6} M VAN and different concentrations of relative foreign species under the chosen conditions. The tolerance concentrations of some metal ions and several biomolecules for the determination of VAN are listed in Table 1. Generally, the tolerance limit is defined as the maximum concentration of other foreign substances that caused a relative error of ±5 %. As is seen in Table 1, the changes of the fluorescence intensity that most ions and biomolecules made were between +5 and −5 % except L-cysteine, whose change of the fluorescence intensity was much larger than 5 % when its concentration was just three times of VAN. This may be due to the thiol group in L-cysteine, which is similar to that of the capping ligands affecting the system. Thus, it is possible to use this method to detect VAN at considerably low concentrations.

Application

In order to check the practicability of the proposed method in food industry, TGA-capped CdTe/ZnS NPs were utilized for VAN detection in practical samples. As mentioned above, VAN exists in most food and drink products, cookie samples were selected to detect the content of VAN here. Standard addition method was adopted in this work and the result is shown in Table 2. From Table 2, we can see that the average recoveries are in an acceptable range of 97.0–102.3 %. Moreover, the relative standard deviation (RSD) was lower than 5 %, which indicated that this method is reliable and feasible for the trace determination of VAN.

Comparison between the present method and some methods reported recently for the determination of VAN is shown in Table 3 [10, 12, 15, 38–40]. From the table we can see that the present method showed a lower detection limit and wider linear range.

Quenching Mechanism

The mechanism of VAN detection based on the quenching of TGA-capped CdTe/ZnS NPs fluorescence intensity is shown in Scheme 1. Herein, we discuss the transfer of electron from CdTe/ZnS NPs to VAN according to previous literatures [41, 42]. Energy transfer, charge transfer and surface adsorbed molecules on the surface of nanoparticles are the most likely quenching mechanisms. As is reported, the band gap of ZnS and CdTe is about 3.6 and 1.5 eV, respectively [43]. The valence band edge of ZnS is below that of CdTe and the conduction band edge of ZnS is above that of CdTe. Upon excitation of TGA-capped CdTe/ZnS NPs, the electrons transfers from the valence band to the conduction band of CdTe and then transfers to the conduction band of ZnS, which results in the formation of a positive charged hole in the valence band and an electron in the conduction band. After recombining of the electron and the hole, a photon is emitted to produce the fluorescence. VAN here acts as the electron acceptor for the electron in conduction band, which prevents the recombination of the electron and the hole at the interfaces of CdTe/ZnS NPs. Thus, a decrease of the fluorescence intensity happens and leads to fluorescence quenching.

Conclusions

In summary, a convenient, sensitive and selective method for the quantitative determination of VAN was established on the basis of the fluorescence quenching of TGA-capped CdTe/ZnS NPs. CdTe/ZnS NPs were successfully synthesized through a wet-chemical method and modified with TGA. Under the optimum conditions, VAN concentrations in the range of 9.4×10^{-7} to 5.2×10^{-4} M was linearly proportional to the relative fluorescence intensity of TGA-capped CdTe/ZnS NPs with a detection limit of 2.6×10^{-7} M. Moreover, interferences of some metal ions and biomolecules were analyzed and most of them had no significant effect on VAN determination. The method was applied to the determination of VAN in cookies and the results were satisfactory. The proposed method provides an approach for VAN determination and it will have a significant impact on the food industry. As CdTe/ZnS NPs have so many advantages, we believe that fluorescence probes based on functionaliazed core-shell CdTe/ZnS NPs will attract more attention in the near future.

Acknowledgments This research is supported by the National Natural Science Foundation of China (NSFC) (No. 21271127, 61171033), the Nano- Foundation of Science and Techniques Commission of Shanghai Municipality (No. 12nm0504200) and the Natural Science Foundation of Shanghai Municipality (No. 13ZR1415600).

References

1. Barghini P, Di Gioia D, Fava F, Ruzzi M (2007) Vanillin production using metabolically engineered Escherichia coli under non-growing conditions. Microb Cell Fact 6:13–23. doi:10.1186/1475-2859-6-13
2. Cava-Roda RM, Taboada-Rodríguez A, Valverde-Franco MT, Marín-Iniesta F (2012) Antimicrobial activity of vanillin and mixtures with cinnamon and clove essential oils in controlling listeria monocytogenes and escherichia coli O157:H7 in milk. Food Bioprocess Technol 5:2120–2131. doi:10.1007/s11947-010-0484-4
3. Waliszewski KN, Pardio VT, Ovando SL (2006) A simple and rapid HPLC technique for vanillin determination in alcohol extract. Food Chem 101:1059–1062. doi:10.1016/j.foodchem.2006.03.004
4. Tai A, Sawano T, Yazama F, Ito H (2011) Evaluation of antioxidant activity of vanillin by using multiple antioxidant assays. Biochim Biophys Acta 1810:170–177. doi:10.1016/j.bbagen.2010.11.004

5. Yoon SH, Li C, Lee YM, Lee SH, Kim SH, Choi MS, Seo WT, Yang JK, Kim JY, Kim SW (2005) Production of vanillin from ferulic acid using recombinant strains of escherichia coli. Biotechnol Bioproc Eng 10:378–384. doi:10.1007/BF02931859
6. Libardi SH, Borges JC, Skibsted LH, Cardoso DR (2011) Deactivation of ferrylmyoglobin by vanillin as affected by vanillin binding to β-lactoglobulin. J Agric Food Chem 59:6202–6208. doi:10.1021/jf1047173
7. Kayaci F, Uyar T (2012) Encapsulation of vanillin/cyclodextrin inclusion complex in electrospun polyvinyl alcohol (PVA) nanowebs: prolonged shelf-life and high temperature stability of vanillin. Food Chem 133:641–649. doi:10.1016/j.foodchem.2012.01.040
8. Hardcastle JL, Paterson CJ, Compton RG (2001) Biphasic sonoelectroanalysis: simultaneous extraction from, and determination of vanillin in food flavoring. Electroanalysis 13:899–905. doi:10.1002/1521-4109(200107)13:11<899::AID-ELAN899>3.0.CO;2-E
9. Farthing D, Sica D, Abernathy C, Fakhry I, Roberts JD, Abraham DJ, Swerdlow P (1999) High-performance liquid chromatographic method for determination of vanillin and vanillic acid in human plasma, red blood cells and urine. J Chromatogr B 726:303–307. doi:10.1016/S0378-4347(99)00031-6
10. Shang L, Zhao FQ, Zeng BZ (2014) Sensitive voltammetric determination of vanillin with an AuPd nanoparticles-graphene composite modified electrode. Food Chem 151:53–57. doi:10.1016/j.foodchem.2013.11.044
11. Ho KL, Chong PP, Yazan LS, Ismail M (2012) Vanillin differentially affects azoxymethane-injected rat colon carcinogenesis and gene expression. J Med Food 15:1096–1102. doi:10.1089/jmf.2012.2245
12. de Jager LS, Perfetti GA, Diachenko GW (2007) Determination of coumarin, vanillin, and ethyl vanillin in vanilla extract products: liquid chromatography mass spectrometry method development and validation studies. J Chromatogr A 1145:83–88. doi:10.1016/j.chroma.2007.01.039
13. Ohashi M, Omae H, Hashida M, Sowa Y, Imai S (2007) Determination of vanillin and related flavor compounds in cocoa drink by capillary electrophoresis. J Chromatogr A 1138:262–267. doi:10.1016/j.chroma.2006.10.031
14. Minematsu S, Xuan GS, Wu XZ (2013) Determination of vanillin in vanilla perfumes and air by capillary electrophoresis. J Environ Sci 25:S8–S14. doi:10.1016/S1001-0742(14)60617-3
15. Bettazzi F, Palchetti I, Sisalli S, Mascini M (2006) A disposable electrochemical sensor for vanillin detection. Anal Chem Acta 555:134–138. doi:10.1016/j.aca.2005.08.069
16. Zheng DY, Hu CG, Gan T, Dang XP, Hu SS (2010) Preparation and application of a novel vanillin sensor based on biosynthesis of Au-Ag alloy nanoparticles. Sensors Actuators B 148:247–252. doi:10.1016/j.snb.2010.04.031
17. Jiang L, Ding YP, Jiang F, Li L, Mo F (2014) Electrodeposited nitrogen-doped graphene/carbon nanotubes nanocomposite as enhancer for simultaneous and sensitive voltammetric determination of caffeine and vanillin. Anal Chim Acta 833:22–28. doi:10.1016/j.aca.2014.05.010
18. Takahashi M, Sakamaki S, Fujita A (2013) Simultaneous analysis of guaiacol and vanillin in a vanilla extract by using high-performance liquid chromatography with electrochemical detection. Biosci Biotechnol Biochem 77:595–600. doi:10.1271/bbb.120835
19. De Jager LS, Perfetti GA, Diachenko GW (2008) Comparison of headspace-SPME-GC-MS and LC-MS for the detection and quantification of coumarin, vanillin, and ethyl vanillin in vanilla extract products. Food Chem 107:1701–1709. doi:10.1016/j.foodchem.2007.09.070
20. Li L, Bian RX, Ding YP, Yu ML, Yu DW (2009) Application of functionalized ZnS nanoparticles to determinate uracil and thymine as a fluorescence probe. Mater Chem Phys 113:905–908. doi:10.1016/j.matchemphys.2008.08.050
21. Tang CR, Su ZH, Lin BG, Huang HW, Zeng YL, Shuang L, Huang H, Wang YJ, Li CX, Shen GL, Yu RQ (2010) A novel method for iodate determination using cadmium sulfide quantum dots as fluorescence probes. Anal Chim Acta 678:203–207. doi:10.1016/j.aca.2010.08.034
22. Dong F, Hu KW, Han HY, Liang JG (2009) A novel method for methimazole determination using CdSe quantum dots as fluorescence probes. Microchim Acta 165:195–201. doi:10.1007/s00604-008-0120-4
23. Fernández-Argüelles MT, Jin WJ, Costa-Fernández JM, Pereiro R, Sanz-Medel A (2005) Surface-modified CdSe quantum dots for the sensitive and selective determination of Cu(II) in aqueous solutions by luminescent measurements. Anal Chem Acta 549:20–25. doi:10.1016/j.aca.2005.06.013
24. Liu MM, Xu L, Cheng WQ, Zeng Y, Yan ZY (2008) Surface-modified CdS quantum dots as luminescent probes for sulfadiazine determination. Spectrochim Acta A 70:1198–1202. doi:10.1016/j.saa.2007.10.040
25. Liang JG, Huang S, Zeng DY, He ZK, Ji XH, Ai XP, Yang HX (2006) CdSe quantum dots as luminescent probes for spironolactone determination. Talanta 69:126–130. doi:10.1016/j.talanta.2005.09.004
26. Peng H, Zhang LJ, Soeller C, Travas-Sejdic J (2007) Preparation of water-soluble CdTe/CdS core/shell quantum dots with enhanced photostability. J Lumin 127:721–726. doi:10.1016/j.jlumin.2007.04.007
27. Wang BB, Shang H, Nie CP, Wang Q, Ma MH, Cai ZX (2013) A novel two-step controlled basic water phase method for synthesizing size-tunable CdTe/$Cd(OH)_2$ core/shell quantum dots with high quantum yield and excellent stability. J Lumin 143:262–270. doi:10.1016/j.jlumin.2013.05.007
28. Sung TW, Lo YL (2012) Highly sensitive and selective sensor based on silica-coated CdSe/ZnS nanoparticles for Cu^{2+} ion detection. Sensors Actuators B 165:119–125. doi:10.1016/j.snb.2012.02.028
29. Zhang H, Zhou Z, Yang B, Gao MY (2003) The influence of carboxyl groups on the photoluminescence of mercaptocarboxylic acid-stabilized CdTe nanoparticles. J Phys Chem B 107:8–13. doi:10.1021/jp025910c
30. Li L, Cheng Y, Ding YP, Gu SQ, Zhang FF, Yu WJ (2013) Synthesis of functionalized core-shell CdTe/ZnS nanoparticles and their application as a fluorescence probe for norfloxacin determination. Eur J Inorg Chem 2013:2564–2570. doi:10.1002/ejic.201201372
31. El-sadek MSA, Babu SM (2010) Growth and optical characterization of colloidal CdTe nanoparticles capped by a bifunctional molecule. Phys B 405:3279–3283. doi:10.1016/j.physb.2010.04.060
32. Chen H, Li RB, Lin L, Guo GS, Lin JM (2010) Determination of L-ascorbic acid in human serum by chemiluminescence based on hydrogen peroxide-sodium hydrogen carbonate-CdSe/CdS quantum dots system. Talanta 81:1688–1696. doi:10.1016/j.talanta.2010.03.024
33. Lin WJ, Costa-Fernández JM, Pereiro R, Sanz-Medel A (2004) Surface-modified CdSe quantum dots as luminescent probes for cyanide determination. Anal Chim Acta 522:1–8. doi:10.1016/j.aca.2004.06.057
34. Baride A, Engebretson D, Berry MT, May PS (2013) Quenching of coumarin emission by CdSe and CdSe/ZnS quantum dots: implications for fluorescence reporting. J Lumin 141:99–105. doi:10.1016/j.jlumin.2013.03.027
35. Gudarzy F, Moghaddam AB, Mozaffari S, Ganjkhanlou Y, Kazemzad M, Zahed R, Bani F (2013) A lanthanide nanoparticle-

based luminescent probe for folic acid. Microchim Acta 180:1257–1262. doi:10.1007/s00604-013-1050-3

36. Azab HA, Duerkop A, Saad EM, Awad FK, Abd El Aal RM, Kamel RM (2012) A novel luminescent terbium-3-carboxycoumarin probe for time-resolved fluorescence sensing of pesticides methomyl, aldicarb and prometryne. Spectrochim Acta A Mol Biomol Spectrosc 97:915–922. doi:10.1016/j.saa.2012.07.079
37. Chen J, Gao YC, Xu ZB, Wu GH, Chen YC, Zhu CQ (2006) A novel fluorescent array formercury (II) ion in aqueous solution with functionalised cadmium selanide nanoclusters. Anal Chim Acta 577:77–84. doi:10.1016/j.aca.2006.06.039
38. Timotheou-Potamia M, Calokerinos AC (2007) Chemiluminometric determination of vanillin in commercial vanillin products. Talanta 71:208–212. doi:10.1016/j.talanta.2006.03.046
39. Ni YN, Zhang GW, Kokot S (2005) Simultaneous spectrophotometric determination of maltol, ethyl maltol, vanillin and ethyl vanillin in foods by multivariate calibration and artificial neural networks. Food Chem 89:465–473. doi:10.1016/j.foodchem.2004.05.037
40. Yardim Y, Gülcan M, Sentürk Z (2013) Determination of vanillin in commercial food product by adsorptive stripping voltammetry using a boron-doped diamond electrode. Food Chem 141:1821–1827. doi:10.1016/j.foodchem.2013.04.085
41. Gao DY, Sheng ZH, Han HY (2010) A novel method for the analysis of calf thymus DNA based on CdTe quantum dots-Ru(bpy)$_3^{2+}$ photoinduced electron transfer system. Microchim Acta 168:341–345. doi:10.1007/s00604-010-0289-1
42. Liu ZQ, Yin PF, Gong HP, Li PP, Wang XD, He YQ (2012) Determination of rifampicin based on fluorescence quenching of GSH capped CdTe/ZnS QDs. J Lumin 132:2482–2488. doi:10.1016/j.jlumin.2012.03.072
43. Wang XN, Liu R, Wang T, Wang BY, Xu Y, Wang H (2013) Dual roles of ZnS thin layers in significant photocurrent enhancement of ZnO/CdTe nanocable arrays photoanode. ACS Appl Mater Interfaces 5:3312–3316. doi:10.1021/am4003793